12th International Conference on Domain Decomposition Methods
Editors: Tony Chan, Takashi Kako, Hideo Kawarada, Olivier Pironneau,

41. Application of the Domain Decomposition Method to the Flow around the Savonius Rotor

Testuya Kawamura[1], Tsutomu Hayashi[2], Kazuko Miyashita[3]

Introduction

In this study, we focus on the Savonius Rotor and try to compute the flow field under its operation and make clear the running performance by means of the numerical simulation. Our final objective is to simulate the flow field around the whole rotor and estimate the effect of the sidewall or the other rotor. Incompressible Navier-Stokes equations are solved in a few regions separately where the fixed coordinate and the rotating coordinate are used respectively. We employ domain decomposition method in order to connect these regions with adequate accuracy. The basic equations in each region are solved by using standard MAC method[HW65]. The physical quantities such as the velocity and the pressure in each region are transferred through the overlapping region, which is common in each domain. Reasonable results are obtained in the present calculations.

Recently, the wind force is widely recognized as the environmentally friendly energy and attracts public attention. The wind power plant using windmills is the typical example. In order to make an effective windmill, it is very important to analyze the flow field around a windmill. In this case, numerical simulation becomes a promising method. The most important part of the investigation is to analyze the flow field near the rotating rotor of the windmill. On the other hand, it is also very important to investigate the interaction among the windmills if they are placed without long distance.

For the numerical simulation of rotating body, it is convenient to use the rotating coordinate system, which rotates with the same speed. However, if there is another body which is not rotating or if there are many rotors which rotate at different position and with different speed, it is very difficult to choose one special rotating coordinate system. In these situations, it is natural to use many coordinate systems separately, which are suitable for the flow simulation around each rotor and connect these coordinates adequately. We focus on these points and simulate the flow fields around a windmill by using domain decomposition method in which the whole computation region is divided into several domains and they are connected adequately.

The Savonius rotor[Sav31] is chosen for the simulation since in this case the rotating bluff body generates the complex flow field with large separation and it is very interesting to investigate such flow from the fluid dynamical point of view. Figure 1 is the schematic figure of the Savonius rotor. The features of this windmill are easy to make, independent of the direction of the wind, low speed and high torque. The Savonius rotor is usually used as the pump.

[1]Ochanomizu University, kawamura@ns.is.ocha.ac.jp
[2]Tottori University, hayashi@damp.tottori-u.ac.jp
[3]Ochanomizu University, miya@ns.is.ocha.ac.jp

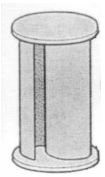

Figure 1: Savonius rotor

There are several experimental and numerical works concerning with Savonius rotor [RESF78] [Oga83] [IST94]. Among them, Ishimatsu et al.[IST94] calculated the flow around a Savonius rotor. Their objective is to compute running performance of one windmill. Therefore, they ignore the effect of the sidewall, ground and other windmills. Their numerical method is based on the finite volume method with unstructured grids. As is discussed above, one of the important objectives of the present study is to investigate the effect of the obstacles. Therefore, we employ the domain decomposition method in this study.

Numerical Method

Since the rotational frequency is low enough, the flow around the Savonius rotor is assumed as incompressible. The basic equations are

$$\nabla \mathbf{v} = 0$$

$$\frac{\partial \mathbf{v}}{\partial t} + (\mathbf{v} \cdot \nabla \mathbf{v}) = -\nabla p + \frac{1}{Re} \nabla^2 \mathbf{v}$$

where Re is the Reynolds number. We use both Cartesian coordinate system (x,y) and

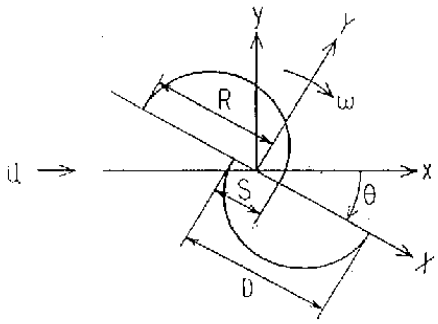

R: radius of rotation
D: bucket diameter
ω: angular velocity
θ: attack angle

Figure 2: Savonius Rotors without walls & obstacle

the rotating coordinate system (X,Y) which rotates around vertical axis with constant angular velocity ω. If we use the symbols indicated in Figure 2, the relation between two coordinate systems is

$$X = x \cos\theta - y \sin\theta,$$

$$Y = x \sin\theta + y \cos\theta,$$

where θ is the angle between two coordinate systems. The basic equations are expressed in the rotating coordinate system as

$$\frac{\partial U}{\partial X} + \frac{\partial V}{\partial Y} = 0$$

$$\frac{\partial U}{\partial t} + U\frac{\partial U}{\partial X} + V\frac{\partial U}{\partial Y} - \omega^2 X + 2\omega V = -\frac{\partial P}{\partial X} + \frac{1}{Re}\left(\frac{\partial^2 U}{\partial X^2} + \frac{\partial^2 U}{\partial Y^2}\right)$$

$$\frac{\partial V}{\partial t} + U\frac{\partial V}{\partial X} + V\frac{\partial V}{\partial Y} - \omega^2 Y - 2\omega U = -\frac{\partial P}{\partial Y} + \frac{1}{Re}\left(\frac{\partial^2 V}{\partial X^2} + \frac{\partial^2 V}{\partial Y^2}\right)$$

where (U,V) are the velocity components in (X,Y) direction while (u,v) are those in the fixed Cartesian coordinate system. These velocity components are connected to each other through the following relations:

$$U = u \cos\theta - v \sin\theta - \omega Y,$$

$$V = u \sin\theta + v \cos\theta + \omega X.$$

We use two computational domains. One domain(region1) includes the rotating rotor and another(region2) includes the fixed walls. Since the shape of the Savonius rotor is semicircular, it is convenient to use a semicircular region. The region including rotors consists of two semicircular regions whose centers are located at different positions. These two regions are connected by one line which passes two centers as is shown in Figure 3. Clearly, it is convenient to use the grid system based on the cylindrical coordinate. Another domain(region2) is rectangular and includes the fixed walls(Figure 4). The Cartesian coordinate system is used and the non-uniform rectangular grid is

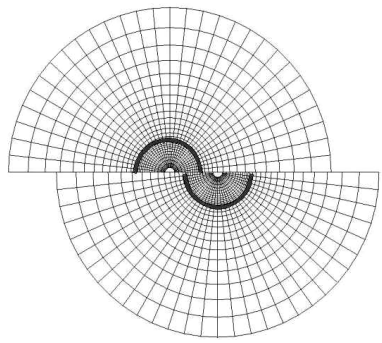

Figure 3: Inner region(region1). The bold lines indicate two blades

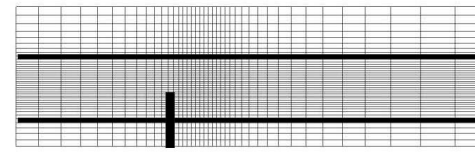

Figure 4: Outer region(region2). The bold lines indicate the sidewalls

employed in this region. The grid points do not coincide with each other in both x(X) and y(Y) direction. The computations in the two domains, which have the overlapping region are performed alternatively at every time step. Figure 5 indicates the whole computational region. The physical quantities (velocity and pressure) are exchanged through the common overlapping region as is shown in Figure 6. When we compute

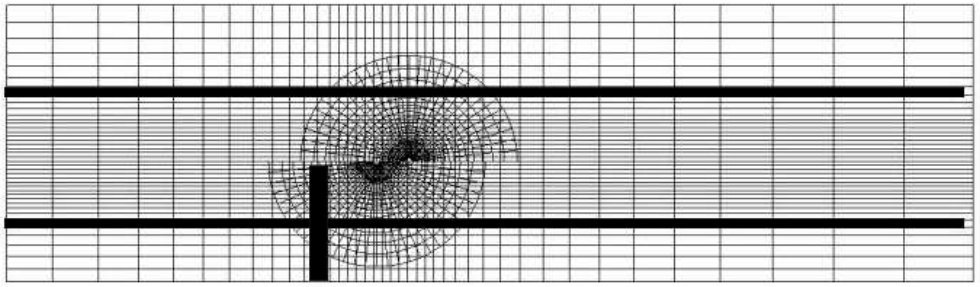

Figure 5: Whole computational region

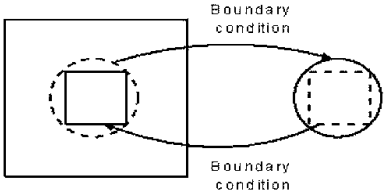

Figure 6: Domain decomposition by the overlapping region

the flow field of region1, the boundary conditions are required on each boundary. If the boundary locates outside of the region, the boundary conditions are determined by the usual way, i.e. free stream condition or something like this. If the boundary locates inside of the region2, the boundary values can be obtained from the computational results of the region2. In this case, some interpolations are required since the grid systems in both regions are different. In this study, the interpolation shown in Figure 7 is used. Since this formula requires only the distance from the four corners

$$f_P = \frac{1}{R}\left(\frac{1}{r_Q}f_Q + \frac{1}{r_R}f_R + \frac{1}{r_S}f_S + \frac{1}{r_T}f_T\right)$$

$$where \;\; R = \frac{1}{r_Q} + \frac{1}{r_R} + \frac{1}{r_S} + \frac{1}{r_T}$$

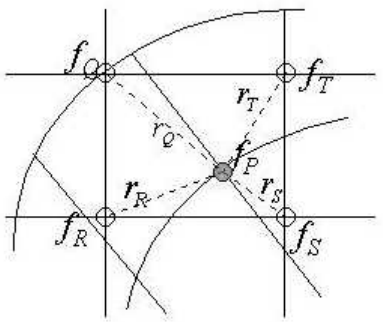

Figure 7: Interpolation in the overlapping region

in one grid cell, it can be used even if the grid cell is highly deformed.

Similar technique is used for determining the boundary conditions of region2 from the computational results of region1. In region1, two regions of semicircular shape are connected through one line without overlapping region. The boundary conditions on

this line are given by the average value of the nearest grid points in each region(Figure 8) as follows: The numerical method to solve incompressible Navier-Stokes equation

$$f_P = (f_Q + (1-r)f_R + rf_S)/2.$$

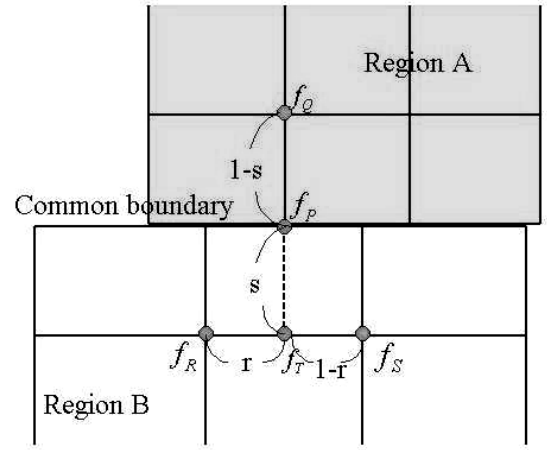

Figure 8: Interpolation along the line

is the standard MAC method. All the spatial derivatives except the nonlinear term of the Navier-Stokes equation is approximated by the second order central difference. Nonlinear terms are approximated by the third order upwind scheme[KK84] due to the numerical stability. Euler explicit scheme is employed for the time integration.

Result

Typical results obtained by the present study are shown here. The dimensionless gap width(=S/D, see Figure 2) is chosen to 0.15 and tip speed ratio $\lambda(= R\omega/u_\infty)$ is changed from 0.25 to 1.25. Figure 9 indicates the initial position of the rotor. In this

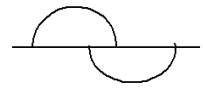

Figure 9: Initial position of the rotor

case, the rotational angle θ is defined as zero and the rotor begins to rotate clockwise from this position. Figure 10 is an example of the instantaneous velocity vectors. Both the vectors in the inner region and the outer region are plotted in the same figure. The vectors vary continuously from the inner region to the outer region, which indicates the interpolation works well in this calculation. Figure 11 is time history of the torque coefficient. The torque coefficient $C_r(= T/qRA$ where T is the torque, q is the dynamic pressure, R is the radius of the rotor, and A is the projection area). The tip speed ratio is 0.25 and no walls exist. Clearly, it has a period of 180 degree. The torque becomes maximum and minimum around 30 and 150 degree respectively and becomes zero around 120 and 180 degree. Figure 12 is also time history of the

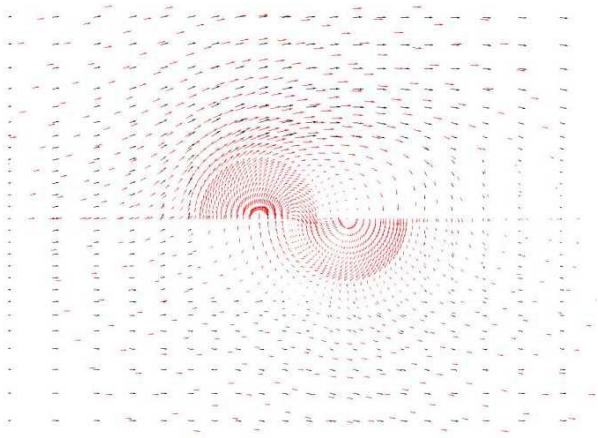

Figure 10: An example of the instantaneous velocity fields in the whole region

torque coefficient but the tip speed ratio is 0.5 and 0.75. As tip speed ratio becomes large, the negative part of the curve becomes large indicating the total torque becomes small. Figure 13 is the result of the calculation with walls. It corresponds to Figure 11 and Figure 12. Although the shape of each curve is similar, the absolute value becomes large for the latter case. Figure 14 is the time-averaged torque coefficient

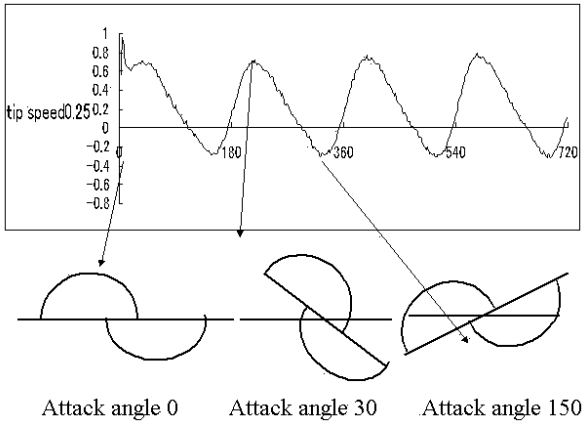

Figure 11: Time history of the torque coefficient without walls(Tip speed ratio is 0.25)

for various tip speed ratio λ. Both the results of the calculations with and without walls are indicated in the same figure. Torque coefficients decrease nearly linear as the tip speed ratio increases and become negative around 0.8. They become almost twice when the walls exist. Figure 15 is the time-averaged power coefficients $C_p(= \lambda C_r)$ for various tip speed ratio. Both the results with and without walls are shown. The power coefficient has its maximum value around $\lambda = 0.5$ and $\lambda = 0.4$ for the case with and without walls respectively. The maximum value is almost twice for the case with

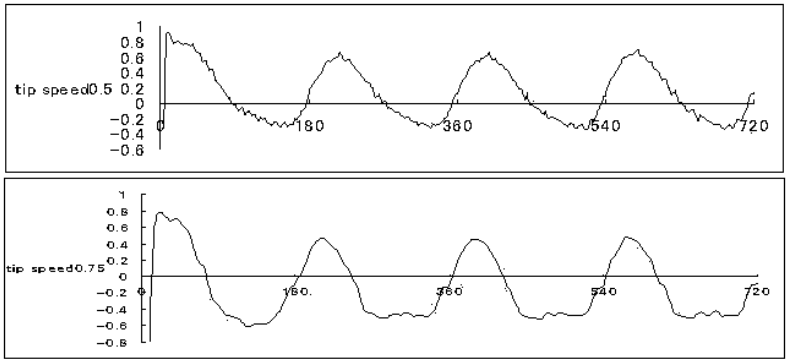

Figure 12: Time history of the torque coefficient without walls(Tip speed ratio is 0.5 and 0.75)

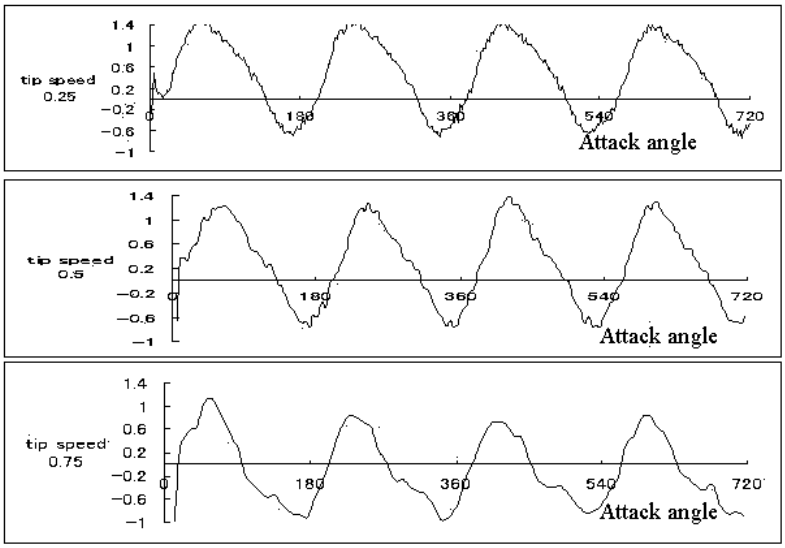

Figure 13: Time history of the torque coefficient with walls(Tip speed ratio is 0.25, 0.5 and 0.75)

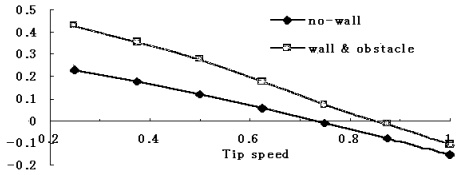

Figure 14: Time-averaged torque coefficient for various tip speed ratios for the cases with and without walls

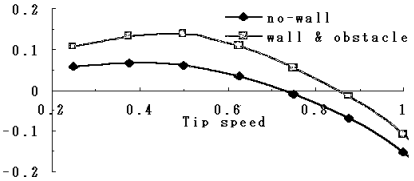

Figure 15: Time-averaged power coefficient for various tip speed ratios for the cases with and without walls

walls.

Summary

In this study, the flow field around the windmill is computed by using domain decomposition method. Although the Savonius rotor is chosen for the present computation, this method can be applied for the computations of other windmills. Two computational domains are used and connected to each other. One domain contains the rotating rotor and rotational coordinate system is employed. Another contains the fixed walls and the Cartesian coordinate system is used. Both regions have common overlapping region. The physical quantities on the boundary of one domain in the overlapping region are calculated by interpolating the physical values at the grid points in another region which are located inside of the region. The running performance of the Savonius rotor such as the torque coefficient and the power coefficient is obtained for various tip speed ratios. The effect of the walls on the running performance is also investigated. It is found that torque coefficient and the power coefficient become almost twice when the walls are placed adequately.

References

[HW65]F. H. Harlow and J. E. Welch. Numerical calculation of time-dependent viscous incompressible flow of fluid with free surface. *Physics of Fluids*, 8(12):2182–2189, December 1965.

[IST94]K. Ishimatsu, T. Shinohara, and F. Takuma. Numerical simulation for savonius rotors(running performance and flow fields). *JSME(B)*, 60(569):154–160, 1994.

[KK84]T. Kawamura and K. Kuwahara. Computation of high Reynolds number flow around a circular cylinder with surface roughness. *AIAA paper*, 84(0340), 1984.

[Oga83]Ogawa. The study on the savonius wind turbine (1st. report; theoretical analysis). *JSME*, 49(441), 1983.

[RESF78]B. F. Blackwell R. E. Sheldahl and L. V. Feltz. Wind tunnel performance data for two- and three-bucket savonius rotors. *J. Energy*, 1978.

[Sav31]S. J. Savonius. The s-roter and its application. *Mech. Eng.*, 53:333, 1931.